Cellular Physiology and Biochemistry

Cell Physiol Biochem 2018;48:407-418
DOI: 10.1159/000491770
Published online: July 17, 2018
Accepted: May 04, 2018

Original Paper

Role of 1α,25-Dihydroxyvitamin D_3 in Adipogenesis of SGBS Cells: New Insights into Human Preadipocyte Proliferation

Ingrid Felicidade[a,b] Daniele Sartori[c] Susan LM Coort[b]
Simone Cristine Semprebon[d] Andressa Megumi Niwa[d]
Gláucia Fernanda Rocha D'Epiro[d] Bruna Isabela Biazi[d] Lilian Areal Marques[d]
Chris T. Evelo[b,e] Mário Sérgio Mantovani[d] Lúcia Regina Ribeiro[a]

[a]São Paulo State University (UNESP), School of Medicine, Department of Pathology, Botucatu, Brazil, [b]Maastricht University, Department of Bioinformatics - BiGCaT, NUTRIM School for Nutrition and Translational Research in Metabolism, Maastricht, The Netherlands, [c]State University of Londrina (UEL), Department of Biochemistry and Biotechnology, Londrina, [d]State University of Londrina (UEL), Department of General Biology, Londrina, Brazil, [e]Maastricht University, Maastricht Centre for Systems Biology (MaCSBio), Maastricht, The Netherlands

Key Words
Adipogenesis • Preadipocyte • SGBS • Vitamin D

Abstract
Background/Aims: Compared with non-obese individuals, obese individuals commonly store more vitamin D in adipose tissue. *VDR* expression in adipose tissue can influence adipogenesis and is therefore a target pathway deserving further study. This study aims to assess the role of $1,25(OH)_2D_3$ in human preadipocyte proliferation and differentiation. ***Methods:*** RTCA, MTT, and trypan blue assays were used to assess the effects of $1,25(OH)_2D_3$ on the viability, proliferation, and adipogenic differentiation of SGBS cells. Cell cycle and apoptosis analyses were performed with flow cytometry, triglycerides were quantified, and RT-qPCR was used to assess gene expression. ***Results:*** We confirmed that the SGBS cell model is suitable for studying adipogenesis and demonstrated that the differentiation protocol induces cell maturation, thereby increasing the lipid content of cells independently of treatment. $1,25(OH)_2D_3$ treatment had different effects according to the cell stage, indicating different modes of action driving proliferation and differentiation. In preadipocytes, $1,25(OH)_2D_3$ induced G1 growth arrest at both tested concentrations without altering *CDKN1A* gene expression. Treatment with 100 nM $1,25(OH)_2D_3$ also decreased MTT absorbance and the lipid concentration. Moreover, increased normalized cell index values and decreased metabolic activity were not induced by proliferation or apoptosis. Exposure to 100 nM $1,25(OH)_2D_3$ induced *VDR*, *CEBPA*, and *CEBPB* expression, even in the preadipocyte stage. During adipogenesis, $1,25(OH)_2D_3$ had

Ingrid Felicidade
Centro de Ciências Bio., Dept. de Bio. Geral, Lab. de Genética Toxicológica, Univ. Estadual de Londrina
Rodovia Celso Garcia Cid, PR 445 Km 380, Campus Universitário. CEP 86057-970, Londrina/PR (Brazil)
Tel. +55 43 3371-5120, Fax +55 43 3371-5120, E-Mail ingrid.felicidade@gmail.com

limited effects on processes such as *VDR* and *PPARG* gene expression, but it upregulated *CEBPA* expression. ***Conclusions:*** We demonstrated for the first time that $1,25(OH)_2D_3$ induces changes in preadipocytes, including *VDR* expression and growth arrest, and increases the lipid content in adipocytes treated for 16 days. Preadipocytes are important cells in adipose tissue homeostasis, and understanding the role of $1,25(OH)_2D_3$ in adipogenesis is a crucial step in ensuring adequate vitamin D supplementation, especially for obese individuals.

Introduction

Vitamin D_3 is synthesized in the skin in response to ultraviolet-B light, and it is then converted in the liver to 25-hydroxyvitamin D_3 ($25(OH)D_3$), which serves as the prohormone for the renal production of the hormone 1α,25-dihydroxyvitamin D_3 ($1,25(OH)_2D_3$) [1]. The bioactive metabolite $1,25(OH)_2D_3$ binds to the vitamin D receptor (VDR) with high affinity, acting as a pleiotropic endocrine hormone and influencing many physiological processes, including gene expression [2-4]. Ligand-bound VDR forms a heterodimeric complex with the retinoid-X receptor and binds to the vitamin D response element in the promoter region of target genes, thereby influencing gene expression [5,6]. In addition, vitamin D_3 exerts VDR-independent non-genomic activity by affecting intracellular signaling molecules [4, 7, 8].

Evidence suggests a strong association between vitamin D deficiency and obesity [9]. The hormone $1,25(OH)_2D_3$ and its metabolites are lipophilic and are stored in adipose tissue, which might explain the low serum levels of this hormone in obese individuals [10,11]. Didriksen et al. [12] demonstrated that after treatment with $1,25(OH)_2D_3$ at 20,000 IU/week for 3–5 years, adipose tissue from obese individuals with impaired glucose tolerance and/or impaired fasting glucose contains six-fold higher $1,25(OH)_2D_3$ levels than adipose tissue from a placebo group.

At the cellular level, the expansion of adipose tissue during obesity development involves a higher number of pre-existing adipocytes (hypertrophy) and an elevated number of adipocytes, which is caused by the increased proliferation and differentiation of preadipocytes [13,14]. Understanding the mechanisms that control the proliferation of preadipocytes and the conversion of preadipocytes to adipocytes can provide new perspectives for understanding etiology and preventing obesity and obesity-associated disorders [15].

Considering the obesity pandemic, interest in the modulation of factors involved in adipogenesis, such as transcription factors [16], has steadily increased. Clemente-Postigo et al. [17] showed that *VDR* expression is higher in adipose tissue from morbidly obese subjects compared to tissue from lean subjects. The increased availability of the ligand-activated transcription factor VDR during adipogenesis and its link with obesity could be indicative of the effect of $1,25(OH)_2D_3$ [9,18].

The aim of the current study is to describe the effects of $1,25(OH)_2D_3$ on the proliferation and differentiation of human preadipocytes. We used human SGBS (Simpson-Golabi-Behmel syndrome) preadipocytes as a model system and treated cells with two concentrations (10 nM and 100 nM) of $1,25(OH)_2D_3$.

Materials and Methods

Cell culture

Human preadipocyte SGBS cells were cultured and allowed to differentiate into mature adipocytes for 16 days, as described previously [19, 20]. To determine the optimal cell density for experiments, a titration assay was performed in a closed-system *xCELLigence* Real Time Cell Analyzer (RTCA) system according to the manufacturer's protocol (Roche Applied Science, Germany). Based on these results, a cell density of 2,000 cells/96-well plate was used in all assays.

Study design

All cells were seeded 24 h prior to the experiment and then divided and treated according to the assay protocol, and all evaluations were performed using three biological replicates. The cells were cultured and differentiated using identical procedures that varied only in the time point at which the cells were treated with 10 nM or 100 nM 1,25(OH)$_2$D$_3$ (Sigma-Aldrich, USA) or with the corresponding fresh medium. Therefore, cells were harvested at the same stage. Single and continuous treatments were performed at different cell stages according to the requirements of each experiment. The following experimental groups (for all online suppl. material, see www.karger.com/doi/10.1159/000491770, Suppl. Fig. S1) were examined.

Single treatments:

i) Pre: single 2-day treatment in preadipocytes (Pre) 24 h after seeding;

ii) Adipocytes: single treatments in differentiated cells, treated at the differentiation stage (T4d) or 4 (T8d), 8 (T12d), or 12 (T16d) days post-differentiation.

Continuous treatments:

iii) Pre-T$_{endpoint}$: treated from the preadipocyte stage until the endpoint of the experiment (Pre-T16d);

iv) T0h-T$_{endpoint}$: treated from the differentiation stage in conjunction with the differentiation medium at T0h, until the endpoint of the experiment (T0h-T16d).

Control:

v) Control: untreated.

Lipid quantification and microscopic analysis

Microscopic analysis and the quantification of triglycerides in treated preadipocytes and adipocytes were performed using AdipoRed™ (Lonza, Switzerland). The assay was performed according to the manufacturer's instructions, and measurements were made on a microplate spectrophotometer (excitation, 485 nm; emission, 535/25 nm; Victor 3, PerkinElmer, USA). Two time points were chosen for lipid quantification: single preadipocyte treatment and continuous treatment from the preadipocyte stage (groups i and iii).

Microscopic analysis was performed using an inverted microscope with a 20× lens at an optical magnification of 460× with conventional (control cells after 16 days of differentiation) and fluorescent light (preadipocytes) (green filter; excitation 482/18 nm; emission 532/59 nm; FLoid® Cell Imaging Station, Life Technologies).

RTCA on an xCELLigence system

The RTCA assay provides real-time monitoring of live cells using electric impedance. Culture plates with projecting arrays of gold microelectrodes at the base of each well allow the measurement of electrical impedance at certain points in the experiment (Zi) relative to the background reading (Z0) to enable the calculation of the arbitrary unit cell index (CI) ($CI = \frac{Zi - Z0}{30}$) [21]. Normalization to the initial reading yields the normalized cell index (NCI). This electrical impedance can be affected by the morphology, adhesion, and mobility of adherent cells and by cell content, including lipids.

RTCA assays were performed according to the manufacturer's instructions in 96-well E-plates (Roche Applied Science, Germany) containing adhesion solution (fibronectin [1 mg/mL] and gelatin [0.05%]). However, after previous assays demonstrated that the cell profiles with adhesion solution were similar to those observed in the absence of adhesion solution after 24 h (data not shown), we decided to use the adhesion solution only for extended treatment (19 days) in the same plate.

MTT assays

The MTT (3-(4,5-dimethylthiazol-2-yl)-2,5-diphenyltetrazolium bromide) cell assay used in this study was based on a protocol described by Mosmann [22]. Applying the same treatment design as the RTCA, the plates were divided to contain the target treatments (preadipocytes, T4d, T8d, T12d, and T16d), single preadipocytes (group i), continuous treatments (groups iii and iv), control treatments (group v), respective vehicle treatments, and blanks. The assays were performed in 96-well plates without adhesion solution. After the treatment period, the contents of the wells were removed and replaced with 100 µL of 0.5 mg/mL MTT diluted with serum-free DMEM. The cells were incubated at 37°C for 4 h, MTT solution was removed, and 100 µL of DMSO was added. Absorbance at 540 nm was measured in a spectrophotometer (Thermoplate).

Trypan blue assay

The trypan blue assay was performed on preadipocytes to further elucidate the profiles determined by the RTCA and MTT assays. This assay was performed only on preadipocytes treated with 1,25$(OH)_2D_3$ or the vehicle for 48 h in 6-well plates. Cell numbers were determined with the trypan blue dye by an automated cell counter (Countess®, Invitrogen).

Real-time quantitative polymerase chain reaction (RT-qPCR)

To evaluate mRNA gene expression, RT-qPCR was performed. The human preadipocytes were treated with the vehicle or 1,25$(OH)_2D_3$ (10 nM or 100 nM) according to the following groups: i) single treatment of preadipocytes (Pre) for 48 h; single treatment of preadipocytes at the differentiation stage (T0h) for ii) 4 h (T0h-T4h) or iii) 24 h (T0h-T24h); and iv) single treatment of adipocytes 11 days after differentiation (T12d) for 24 h.

The following genes were selected from the literature based on the pathways involved: vitamin D receptor (*VDR)*, transcription factors related to adipogenesis (*CEBPA*, *CEBPB*, *CEBPD*, *PPARG*), regulatory genes of 1,25$(OH)_2D_3$-mediated apoptosis (*CAPN1*, *BCL2*, *CASP3*, *CASP9*), and the cell cycle (*CDKN1A*); *RPL13A* was considered a housekeeping gene. Primer sequences are shown in (see online suppl. material) Suppl. Table S1, and *CEBPA*, *CEBPB*, *CEBPD*, and *CASP9* were not evaluated at T12d. Total RNA was extracted, and the concentration and integrity were evaluated as described by Baranoski et al. [23] cDNA synthesis was performed as described by Felicidade et al. [24]. RT-qPCR was performed using Platinum SYBR Green qPCR Supermix-UDG (Invitrogen) in a CFX96 Real-Time System (Bio-Rad, USA).

Cell apoptosis and cell cycle analysis

The samples were analyzed by flow cytometry (Accuri C6, BD Pharmingen, USA) using BD Accuri C6 software according to the manufacturer's protocol. For cell apoptosis and cell cycle analysis, the cells received a single treatment of 1,25$(OH)_2D_3$ or the vehicle at the preadipocyte (Pre) stage, at T0h (T0h-$T_{endpoint}$), and 11 days after differentiation (T12d). Moreover, for cell cycle analysis, the T12d treatment and the T12d analysis after each single treatment (preadipocytes and T0h) were not performed because pilot studies showed no difference in the mature adipocyte cell cycle (data not shown). After treatment, the cells were analyzed as follows: i) single treatment of preadipocytes for 48 h (Pre) and 24 h (Pre-T72h), 48 h (Pre-T96h), and 12 days after differentiation (Pre-T12d; in apoptosis analysis); ii) T0h: 4 h (T0h-T4h), 24 h (T0h-T24h), 48 h (T0h-T48h), and 12 days after differentiation (T0h-T12d; in apoptosis analysis); and, for apoptosis analysis, iii) T12d: 11 days after differentiation for 24 h (T12d).

After the treatment period, apoptosis analysis was performed using the Annexin V-PE Apoptosis Detection Kit (BD Pharmingen, USA) according to the manufacturer's protocol. Three cell populations were defined after labeling with fluorochromes as follows: viable cells (Annexin V/7-AAD negative), initial apoptosis (Annexin V positive/7-AAD negative), and final apoptosis/necrosis (Annexin V/7-AAD positive).

For cell cycle analysis, after treatment, the cells were detached from plates using trypsin (Gibco, Thermo Fisher Scientific, USA) and processed as described by Marques et al. [25].

A total of 10,000 events was acquired for each sample, and three experiments were conducted for both analyses.

Statistical analysis

Results are presented as the mean ± SEM. Data from RTCA, MTT, and trypan blue assays, cell apoptosis and cell cycle analyses, and lipid quantification were analyzed by analysis of variance (ANOVA) followed by Dunnett's test to compare the results of the 1,25$(OH)_2D_3$ treatments with those of the control or vehicle treatments using GraphPad Prism 5.0 (GraphPad Software, USA). RT-qPCR fold changes were normalized and calculated as described by Pfaffl et al. [26], using the pairwise method fixed reallocation randomization test in REST software (QIAGEN, 2009, Germany). Student's *t*-test was used to test the difference between treatments (in the cell apoptosis and cell cycle analyses and in RT-qPCR) and between preadipocytes and mature adipocytes (lipid quantification). Statistical analysis was considered significant at $p < 0.05$ for all treatments.

Results

In our cell culture model, the differentiation of human SGBS [19,20] preadipocytes into mature adipocytes was confirmed by the presence of intracellular fat vacuoles (Fig. 1A). In addition, intracellular lipid content was measured in preadipocytes and in untreated (control) differentiated cells or in differentiated cells treated with vehicle (ethanol), 10 nM $1,25(OH)_2D_3$, or 100 nM $1,25(OH)_2D_3$.

We observed elevated intracellular triglyceride levels for all treatments, especially for the $1,25(OH)_2D_3$ treatments, which resulted in significantly increased lipid content compared to the vehicle (Fig. 1B). This finding confirms the effects of $1,25(OH)_2D_3$ on human SGBS preadipocyte cells.

Because $1,25(OH)_2D_3$ can modulate preadipocyte and adipocyte metabolism, we evaluated the treatments at all cell stages and timepoints (single or continuous treatments) and evaluated the NCI and metabolic activity of cells using the RTCA and MTT assays, respectively.

The NCI can be affected by several cellular properties, including adhesion force, motility, and morphological changes. The NCI was similar between $1,25(OH)_2D_3$ treatments (Fig. 2). During proliferation (preadipocyte stage), all treatments showed an increase in NCI; this increase in NCI was especially significant for cells treated with 100 nM $1,25(OH)_2D_3$ (see online suppl. material, Suppl. Fig. S2 and Fig. 2). After the induction of differentiation (T0h), we observed the following three major profiles, which were similar to those observed by Berger et al. [27]: (i) the NCI initially decreased substantially, mainly because of a reduction in cell size without a decrease in proliferation, which was revealed by the proliferation assay and cell apoptosis analysis (Fig. 2; see online suppl. material, Suppl Fig. S3-S4); (ii) the NCI began to increase because of an increase in cell size, and cells began to enter the first phase of cell cycle arrest (T0h-T4d) (Fig. 2; see online suppl. material, Suppl. Fig. S5), which is necessary for preadipocyte differentiation; and (iii) the NCI decreased because of an increase in lipid accumulation in the cells (Fig. 2; Fig. 1), which alters the cell density and reduces adhesion forces. The same adhesion profile observed after the single treatment of

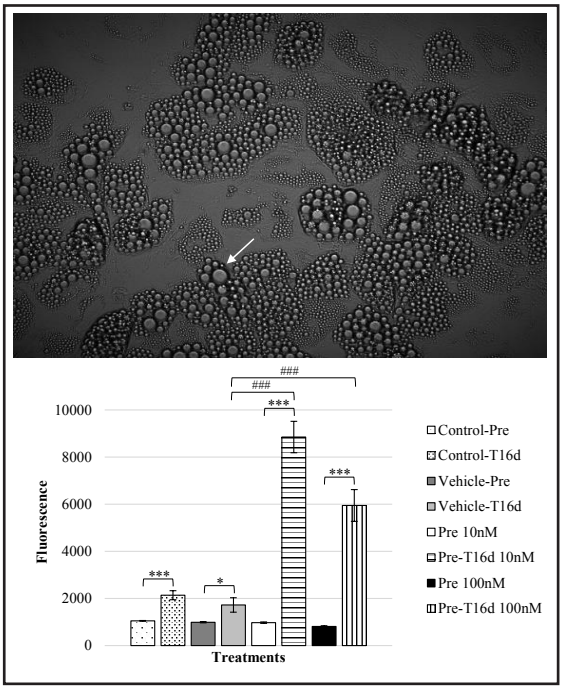

Fig. 1. Human adipocytes after the induction of differentiation. (A) Light microscopic images of mature adipocytes after 16 days of differentiation and (B) lipid quantification in preadipocytes (Pre) and adipocytes treated continuously from the preadipocyte stage (Pre-T16d). (A) Magnification, 460×. The arrow indicates intracellular triglycerides. (B) Student's t-test was used to assess significant differences between preadipocytes and mature adipocytes (*), and ANOVA was used to test significant differences between $1,25(OH)_2D_3$ treatments. Dunnett's test was used to compare findings with vehicle results after 16 days of differentiation (#). Data are presented as the mean ± SEM. *$p<0.05$ and ***/$^{###}p<0.001$. 10 nM and 100 nM: $1,25(OH)_2D_3$ concentrations; control: untreated cells; vehicle: cells treated with ethanol; Pre: cells treated only during the preadipocyte stage; Pre-T16d: cells treated continuously from the preadipocyte stage; T16d: cells treated 16 days after differentiation. All cells were differentiated at the same time, and differentiation proceeded equally among treatments for 16 days.

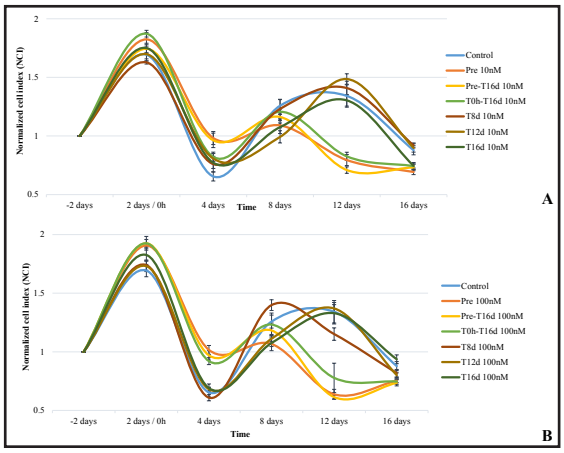

Fig. 2. Normalized cellular index curve. Treatment of human preadipocytes and adipocytes with (A) 10 nM $1,25(OH)_2D_3$ and (B) 100 nM $1,25(OH)_2D_3$ induced proliferation for 16 days. The data are presented as the mean ± SEM. 10 nM and 100 nM: $1,25(OH)_2D_3$ concentrations; control: untreated cells; Pre: cells treated only during the preadipocyte stage; Pre-T16d: cells treated continuously from the preadipocyte stage; T0h-T16d: cells treated continuously from the differentiation stage (T0h); T4d: cells treated only 4 days after differentiation; T8d: cells treated only 8 days after differentiation; T12d: cells treated only 12 days after differentiation. All cells were differentiated at the same time, and differentiation proceeded equally among treatments for 16 days.

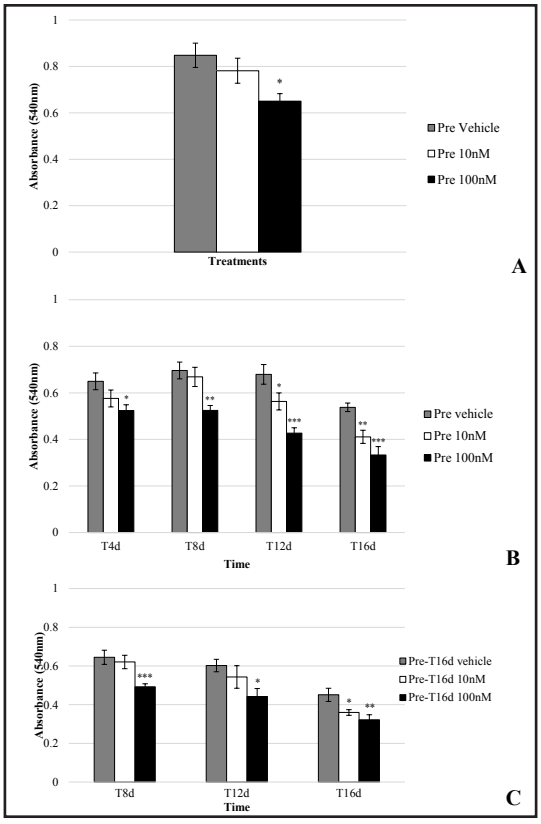

Fig. 3. MTT cell viability assay of (A) preadipocytes treated for 48 h, (B) adipocytes induced to differentiate after a single preadipocyte treatment, and (C) adipocytes treated continuously from the preadipocyte stage. The data are presented as the mean ± SEM. ANOVA was used to test significant differences between treatments, and Dunnet's test was used to compare results with those of the vehicle treatment. The data are presented as the mean ± SEM. *p<0.05, **p<0.01, and ***p<0.001. 10 nM and 100 nM: $1,25(OH)_2D_3$ concentrations; vehicle: cells treated with ethanol; Pre: cells treated only during the preadipocyte stage; Pre-T16d: cells treated continuously from the preadipocyte stage. All cells were differentiated at the same time, and differentiation proceeded equally among treatments for 16 days.

preadipocytes was observed for continuously treated preadipocytes and for preadipocytes treated from T0h (Fig. 2), i.e., the cells showed an increase in NCI compared with the control during the preadipocyte stage and the first 4 days after differentiation, and they showed a decrease from T8d onwards. The NCI of these cells decreased significantly with $1,25(OH)_2D_3$ treatments at T12d and T16d compared with the control (see online suppl. material, Suppl. Fig. S2; Fig. 2). The lipid accumulation results (Fig. 1B) are consistent with the NCI profile in cells treated continuously from the preadipocyte stage (Pre-T16d); at T16d, these cells exhibited the lowest NCI, which is associated with high levels of lipids droplets.

The hormone $1,25(OH)_2D_3$ acted on preadipocytes. A decrease in metabolic activity was observed in single preadipocyte treatments with 100 nM $1,25(OH)_2D_3$ (Fig. 3A) even

after 16 days of differentiation (Fig. 3B), whereas treatment with 10 nM $1,25(OH)_2D_3$ led to a decrease in metabolic activity at only T12d and T16d compared with the vehicle treatment. These results suggest a cumulative effect of $1,25(OH)_2D_3$ treatment (Fig. 3B). Any effect on metabolic activity was observed when the preadipocytes were treated continuously from the differentiation stage (T0h) (see online suppl. material, Suppl. Fig. S6), whereas continuous $1,25(OH)_2D_3$ treatment from the preadipocyte stage had effects similar to those of the single preadipocyte treatments (Fig. 3C). Adipocytes obtained from T0h until 16 days after differentiation appeared to show decreased sensitivity to $1,25(OH)_2D_3$ treatment (see online suppl. material, Suppl. Fig. S6).

Furthermore, we observed a decrease in fluorescence in cells subjected to $1,25(OH)_2D_3$ treatment during the preadipocyte stage (Fig. 4A). Subtle differences in cell morphology were also observed between $1,25(OH)_2D_3$ -treated cells and vehicle-treated or control cells; $1,25(OH)_2D_3$-treated cells were more elongated and showed the characteristics of fibroblasts (compared to control and vehicle), which could be consistent with the increase in NCI (Fig. 4A; Fig. 2). The results of the image analysis and the decreased MTT absorbance values revealed that 100 nM $1,25(OH)_2D_3$ decreased intracellular lipid levels (Fig. 4B), indicating a possible decrease in metabolic activity.

The ability of $1,25(OH)_2D_3$ to induce growth arrest has been widely studied in cancer cells, but it was observed here for the first time in human preadipocytes. Human preadipocyte cells demonstrated G1 growth arrest after $1,25(OH)_2D_3$ treatment, which also decreased the number of cells in the S phase (Fig. 4C). In addition, the increase in cells in the G2 phase

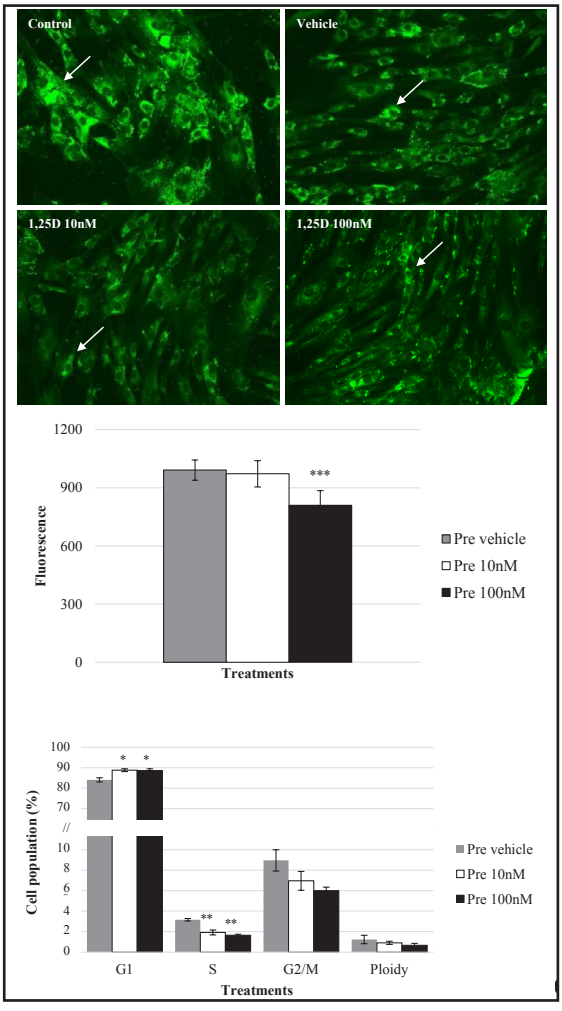

Fig. 4. Results of $1,25(OH)_2D_3$ treatment of human preadipocytes for 48 h. (A) Fluorescence microscopy analysis, (B) lipid quantification, and (C) cell cycle analyses. ANOVA was used to test significant differences between treatments, and Dunnet's test was used to compare results with those of the vehicle treatment. The data are presented as the mean ± SEM. *p<0.05, **p<0.01, and ***p<0.001. Control: untreated cells; vehicle: cells treated with ethanol; 1,25D: $1,25(OH)_2D_3$; Pre: cells treated only during the preadipocyte stage for 48 h; 10 nM and 100 nM: $1,25(OH)_2D_3$ concentrations.

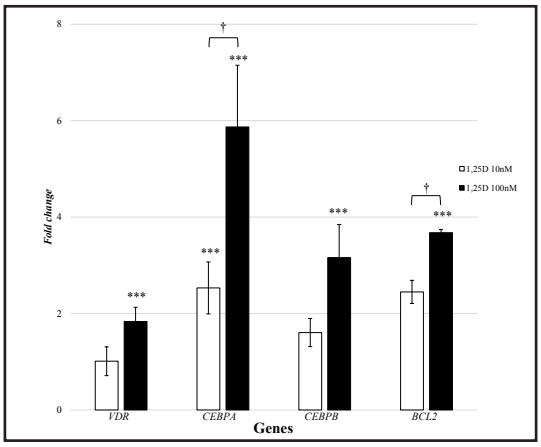

Fig. 5. Effects of $1,25(OH)_2D_3$ on human preadipocyte gene expression. The data are presented as the mean ± SEM. REST software was used to calculate significant differences between normalized fold changes. Student's t-test was used to test significant differences between $1,25(OH)_2D_3$ concentrations. 1,25D: $1,25(OH)_2D_3$. ***p<0.001, and †p ≤ 0.065.

observed in our cell cycle analysis after the induction of differentiation is associated with mitotic clonal expansion. This observation is common in murine cells and is consistent with the NCI profile observed (see online suppl. material, Suppl. Fig. S5; Fig. 2).

To confirm the effects of $1,25(OH)_2D_3$ on human preadipocytes, we evaluated the expression of *VDR* and genes associated with adipogenesis. Treatment with 100 nM $1,25(OH)_2D_3$ upregulated the expression of *VDR*, and this is the first observation of this effect in human preadipocytes; this treatment also upregulated *CEBPA* and *CEBPB*, which are transcription factors involved in adipogenesis (Fig. 5). Consistent with the proliferation assay and cell apoptosis analysis, *BCL2* was upregulated in the 100 nM $1,25(OH)_2D_3$ treatment (Fig. 5). In cells induced to differentiate, RT-qPCR showed significant upregulation of *CEBPA* expression 24 h after treatment with 10 nM $1,25(OH)_2D_3$ ($p = 0.037$) and a trend toward further upregulation at 100 nM $1,25(OH)_2D_3$ ($p = 0.063$) (see online suppl. material, Supple. Fig. S7B). Any changes in gene expression were observed in preadipocytes treated and differentiated for 4 h and in adipocytes treated 11 days after differentiation (see online suppl. material, Suppl. Fig. S7B and S7D).

Discussion

Subcutaneous adipose tissue (SAT), the largest adipose tissue depot in humans, is the preferred site for the storage of excess fat and a target organ for $1,25(OH)_2D_3$ [28]. Obesity was recently demonstrated to be a risk factor associated with vitamin D_3 deficiency [29, 30], which could result from the sequestration or volumetric dilution of vitamin D_3 in adipose tissue [31-33]. Because adipose tissue expresses *VDR*, mainly during differentiation, and because it expresses metabolizing enzymes, e.g., *CYP27B1* and *CYP24A1*, studying the role of $1,25(OH)_2D_3$ in human adipocytes at different stages is a relevant field of study, especially because vitamin D_3 deficiency (including $1,25(OH)_2D_3$ deficiency) and obesity have reached epidemic proportions [18, 28, 33, 34].

In previous studies, adipocyte differentiation was mostly studied in immortalized rodent preadipocyte cell lines, which are aneuploid and are therefore unable to represent complex human mechanisms. Newly isolated human preadipocytes have also been used; although diploid, these cells exhibit donor-dependent variability and limited viability [15]. To overcome these problems, we studied the effects of $1,25(OH)_2D_3$ on the proliferation and differentiation of SGBS preadipocytes. These cells represent a non-immortalized and unprocessed human cell line that maintains good homogeneity between passages [20].

We confirmed that the SGBS cell model was suitable for studying adipogenesis because this model revealed the essential cell characteristics of each stage, including ploidy and mitotic clonal expansion. Our results also demonstrated that the protocol for differentiation

induced cell maturation, and after 16 days, the cells showed significantly increased lipid content independent of treatment.

In this study, we investigated the effects of $1,25(OH)_2D_3$ on human preadipocyte and mature adipocyte proliferation and adipogenesis (differentiation) using SGBS cells. $1,25(OH)_2D_3$ was confirmed to play a role in preadipocyte proliferation; preadipocytes were the main target of $1,25(OH)_2D_3$ activity in this study.

Differences in $1,25(OH)_2D_3$ treatment yielded varying effects according to cell stage, which indicates different modes of action driving proliferation and differentiation. While the differentiation stage has been well studied *in vitro* and in *in vivo* animal models, the proliferation of preadipocytes remains poorly investigated [15].

The cells were seeded at a density established prior to the RTCA assay; this density demonstrated an appropriate proliferation rate to evaluate the proliferation stage and was consistent with the study by Dahl [35]. Our study is the first to also evaluate the real-time proliferation and differentiation of human preadipocytes using SGBS cells via the *xCELLigence* system, and we demonstrated measurable changes in preadipocytes subjected to $1,25(OH)_2D_3$ treatment (see online suppl. material, Suppl. Fig. S2 and Fig. 2).

In preadipocytes, both concentrations of $1,25(OH)_2D_3$ induced G1 growth arrest with a consequent decrease in the percentage of the cell population in the S phase without alteration in *CDKN1A* gene expression (see online suppl. material, Suppl. Fig. S7A). Growth arrest was followed by decreased MTT absorbance and lipid concentration in cells treated with 100 nM $1,25(OH)_2D_3$. Increased NCI values and decreased metabolic activity were not induced by proliferation or apoptosis. Gene expression analysis revealed no changes in caspase expression (see online suppl. material, Suppl. Fig. S7A), although *BCL2* expression increased significantly in cells treated with 100 nM $1,25(OH)_2D_3$. In addition, 100 nM $1,25(OH)_2D_3$ induced *VDR*, *CEBPA*, and *CEBPB* expression, even at the preadipocyte stage. During adipogenesis, $1,25(OH)_2D_3$ had limited effects on *VDR* and *PPARG* gene expression, but it upregulated *CEBPA* expression (see online suppl. material, Suppl. Fig. S7B). We also observed that the NCI of cells treated with 100 nM $1,25(OH)_2D_3$ during the adipogenesis stage increased without any changes in MTT measurements. As expected, differentiated adipocytes demonstrated less sensitivity to $1,25(OH)_2D_3$ treatment compared with preadipocytes, which could be the result of a known decrease in *VDR* expression in adipocytes [16].

The ability of $1,25(OH)_2D_3$ to induce growth arrest has been widely studied in cancer cells, such as ovarian, prostate, breast, and gastric cancer cells [36-39], but this is the first report of this effect in human preadipocytes.

Human preadipocytes are fibroblast-like cells that constitute 15–50% of the cells in adipose tissue [20, 40, 41]. The main role of preadipocytes is to differentiate into functional mature adipocytes to improve insulin sensitivity and avoid ectopic fat deposition, which are associated with insulin resistance, metabolic syndrome, and cardiovascular disease [42]. Preadipocyte differentiation follows a well-established program: i) preadipocytes enter a state of growth arrest, ii) growth-arrested preadipocytes synchronously re-enter the cell cycle and undergo mitotic clonal expansion when induced to differentiate, iii) cells proceed through one or two rounds of the cell cycle, and iv) the induction of a gene expression cascade produces the adipocyte phenotype [43]. The first transcription factors expressed during adipogenesis are *CEBPB* and *CEBPD*, followed by *PPARG* and *CEBPA* [44].

Our data cannot prove that $1,25(OH)_2D_3$ promotes preadipocyte differentiation [18, 34]. However, the observed decrease in NCI at T16d in cells treated continuously from the preadipocyte stage and from T0h (Fig. 2 and see online suppl. material, Suppl.Fig. S2E) is consistent with the results of Berger et al. [27], which demonstrated that cell adhesive forces decrease due to changes in lipid content. Lipid quantification analysis further confirmed that cells treated from the preadipocyte stage contained more triglycerides than control and vehicle-treated cells (Fig. 1B).

Furthermore, treatment with 100 nM $1,25(OH)_2D_3$ induced changes in human preadipocyte proliferation via mechanisms similar to those described for preadipocyte differentiation, specifically growth arrest and changes in the primary transcription factors

of adipogenesis. Moreover, growth arrest was demonstrated to increase cell adhesion forces and cell size, which are both consistent with the observed increase in NCI (Fig. 2 and see online suppl. material, Suppl. Fig. S2) [27]. The decrease in MTT values (Fig. 3) was unrelated to cell death/apoptosis or to decreased cell proliferation (Fig. 4C, and see online suppl. material, Suppl. Fig. S3-S5). Because reductions in MTT are NADH- and NAD(P)H-dependent, decreases in metabolic activity are followed by impairments in reduction rate [23], as verified by the impaired uptake of lipids observed in preadipocytes treated with 100 nM $1,25(OH)_2D_3$ (Fig. 4C). Insulin is necessary to induce adipogenesis and lipogenesis, partly because *PPARG* is activated in the presence of insulin [27]. As demonstrated by our results, *PPARG* expression was not induced in preadipocytes, possibly because of the absence of insulin in the growth medium.

We demonstrated for the first time that $1,25(OH)_2D_3$ induces changes in preadipocytes, including *VDR* expression and growth arrest, and increases the lipid content of adipocytes treated for 16 days. Preadipocytes are important cells in adipose tissue homeostasis, and understanding the role of $1,25(OH)_2D_3$ in adipogenesis is a crucial step to ensure adequate $1,25(OH)_2D_3$ supplementation, especially among obese individuals. Further studies on human preadipocytes treated with $1,25(OH)_2D_3$ are necessary to confirm the mechanisms observed and elucidate the mechanisms of $1,25(OH)_2D_3$ activity in adipose tissue.

Acknowledgements

We thank Dr. Martin Wabitsch and Dr. Pamela Fisher-Posovsky for generously donating the SGBS cells, for helping us improve the protocol, and for providing information about the cells. This study was supported by CAPES (Proc. nº 9933/2014-00), CNPq (Proc. nº 150067/2017-8), and FINEP.

Disclosure Statement

The authors declare to have no conflict of interests.

References

1 Drezner MK, Harrelson JM: Newer knowledge of vitamin D and its metabolites in health and disease. Clin Orthop 1979;139:206-231.
2 Whitfield GK, Hsieh JC, Jurutka PW, Selznick SH, Haussler CA, MacDonald PN, Haussler MR: Genomic actions of 1,25-dihydroxyvitamin D3. J Nutr 1995;125:1690S-4.
3 Jones G, Strugnell SA, DeLuca HF: Current understanding of the molecular actions of vitamin D. Physiol Rev 1998;78:1193-1231.
4 Carlberg C, Campbell MJ: Vitamin D receptor signaling mechanisms: integrated actions of a well-defined transcription factor. Steroids 2013;78:127-136.
5 Carlberg C, Polly P: Gene regulation by vitamin D3. Crit Rev Eukaryot Gene Expr 1998;8:19-42.
6 Carlberg C, Molnar F: Current status of vitamin D signaling and its therapeutic applications. Curr Top Med Chem 2012;12:528-547.
7 Haussler MR, Haussler CA, Jurutka PW, Thompson PD, Hsieh JC, Remus LS, Selznick SH, Whitfield GK: The vitamin D hormone and its nuclear receptor: molecular actions and disease states. J Endocrinol 1997;154:S57-73.
8 Haussler MR, Jurutka PW, Mizwicki M, Norman AW: Vitamin D receptor (VDR)-mediated actions of 1α,25(OH)2 vitamin D3: genomic and non-genomic mechanisms. Best Pract Res Clin Endocrinol Metab 2011;25:543-559.
9 Wood RJ: Vitamin D and adipogenesis: new molecular insights. Nutr Rev 2008;66:40-46.

10 Kamei Y, Kawada T, Kazuki R, Ono T, Kato S, Sugimoto E: Vitamin D receptor gene expression is up-regulated by 1,25-dihydroxyvitamin D3 in 3T3-L1 preadipocytes. Biochem Biophys Res Commun 1993;193:948-955.
11 Marcotorchino J, Tourniaire F, Landrier JF: Vitamin D, adipose tissue, and obesity. Horm Mol Biol Clin Investig 2013;15:123-128.
12 Didriksen A, Burild A, Jakobsen J, Fuskevåg OM, Jorde R: Vitamin D3 increases in abdominal subcutaneous tissue after supplementation with vitamin D3. Eur J Endocrinol 2015;172:235-241.
13 Chawla A, Nguyen KD, Goh YP: Macrophage-mediated inflammation in metabolic disease. Nat Rev Immunol 2011;11:738-749.
14 Moreno-Navarrete JM, Fernández-Real JM: Adipocyte differentiation; in Symonds M (eds): Adipose tissue biology. Springer, New York, 2012, pp 17-28.
15 Alvarez MS, Fernandez-Alvarez A, Cucarella C, Casado M: Stable SREBP 1a knockdown decreases the cell proliferation rate in human preadipocyte cells without inducing senescence. Biochem Biophys Res Commun 2014;447:51-56.
16 Lahnalampi M, Heinäniemi M, Sinkkonen L, Wabitsch M, Carlberg C: Time-resolved expression profiling of the nuclear receptor superfamily in human adipogenesis. PLoS One 2010;5:e12991.
17 Clemente-Postigo M, Muñoz-Garach A, Serrano M, Garrido-Sánchez L, Bernal-López MR, Fernández-García D, Moreno-Santos I, Garriga N, Castellano-Castillo D, Camargo A, Fernández-Real JM, Cardona F, Tinahones FJ, Macías-González M: Serum 25-hydroxyvitamin D and adipose tissue vitamin D receptor gene expression: relationship with obesity and type 2 diabetes. J Clin Endocrinol Metab 2015;100:E591-5.
18 Narvaez CJ, Simmons KM, Brunton J, Salinero A, Chittur SV, Welsh JE: Induction of STEAP4 correlates with 1,25-dihydroxyvitamin D3 stimulation of adipogenesis in mesenchymal progenitor cells derived from human adipose tissue. J Cell Physiol 2013;228:2024-2036.
19 Fischer-Posovszky P, Newell FS, Wabitsch M, Tornqvist H: Human SGBS cells - a unique tool for studies of human fat cell biology. Obes Facts 2008;1:184-189.
20 Wabitsch M, Brenner RE, Melzner I, Braun M, Möller P, Heinze E, Debatin KM, Hauner H: Characterization of a human preadipocyte cell strain with high capacity for adipose differentiation. Int J Obes Relat Metab Disord 2001;25:8-15.
21 Kramer AH, Joos-Vandewalle J, Edkins AL, Frost CL, Prinsloo E: Real-time monitoring of 3T3-L1 preadipocyte differentiation using a commercially available electric cell-substrate impedance sensor system. Biochem Biophys Res Commun 2014;443:1245-1250.
22 Mosmann T: Rapid colorimetric assay for cellular growth and survival: application to proliferation and cytotoxicity assays. J Immunol Methods 1983;65:55-63.
23 Baranoski A, Tempesta OM, Semprebon SC, Niwa AM, Ribeiro LR, Mantovani MS: Effects of sulfated and non-sulfated β-glucan extracted from Agaricus brasiliensis in breast adenocarcinoma cells - MCF-7. Toxicol Mech Methods 2015;13:1-8.
24 Felicidade I, Marcarini JC, Carreira CM, Amarante MK, Afman LA, Mantovani MS, Ribeiro LR: Changes in gene expression in PBMCs profiles of PPARα target genes in obese and non-obese individuals during fasting. Ann Nutr Metab 2015;66:19-25.
25 Marques LA, Semprebon SC, Niwa AM, D'Epiro GF, Sartori D, de Fátima Â, Ribeiro LR, Mantovani MS: Antiproliferative activity of monastrol in human adenocarcinoma (MCF-7) and non-tumor (HB4a) breast cells. Naunyn Schmiedebergs Arch Pharmacol 2016;389:1279-1288.
26 Pfaffl MW, Horgan GW, Dempfle L: Relative expression software tool (REST©) for group-wise comparison and statistical analysis of relative expression results in real-time PCR. Nucleic Acids Res 2002;30:e36.
27 Berger E, Héraud S, Mojallal A, Lequeux C, Weiss-Gayet M, Damour O, Géloën A: Pathways commonly dysregulated in mouse and human obese adipose tissue: FAT/CD36 modulates differentiation and lipogenesis. Adipocyte 2015;4:161-180.
28 Holick MF. The vitamin D epidemic and its health consequences. J Nutr 2005;135:2739S-48.
29 Pourshahidi LK: Vitamin D and obesity: current perspectives and future directions. Proc Nutr Soc 2015;74:115-124.

30 Vimaleswaran KS, Berry DJ, Lu C, Tikkanen E, Pilz S, Hiraki LT, Cooper JD, Dastani Z, Li R, Houston DK, Wood AR, Michaëlsson K, Vandenput L, Zgaga L, Yerges-Armstrong LM, McCarthy MI, Dupuis J, Kaakinen M, Kleber ME, Jameson K, Arden N, Raitakari O, Viikari J, Lohman KK, Ferrucci L, Melhus H, Ingelsson E, Byberg L, Lind L, Lorentzon M, Salomaa V, Campbell H, Dunlop M, Mitchell BD, Herzig KH, Pouta A, Hartikainen AL; Genetic Investigation of Anthropometric Traits-GIANT Consortium, Streeten EA, Theodoratou E, Jula A, Wareham NJ, Ohlsson C, Frayling TM, Kritchevsky SB, Spector TD, Richards JB, Lehtimäki T, Ouwehand WH, Kraft P, Cooper C, März W, Power C, Loos RJ, Wang TJ, Järvelin MR, Whittaker JC, Hingorani AD, Hyppönen E: Causal relationship between obesity and vitamin D status: bi-directional Mendelian randomization analysis of multiple cohorts. PLoS Med 2013;10:e1001383.

31 Wortsman J, Matsuoka LY, Chen TC, Lu Z, Holick MF: Decreased bioavailability of vitamin D in obesity. Am J Clin Nutr 2000;72:690-693.

32 Drincic AT, Armas LA, Van Diest EE, Heaney RP: Volumetric dilution, rather than sequestration best explains the low vitamin D status of obesity. Obesity (Silver Spring) 2012;20:1444-1448.

33 Wamberg L, Christiansen T, Paulsen SK, Fisker S, Rask P, Rejnmark L, Richelsen B, Pedersen SB: Expression of vitamin D-metabolizing enzymes in human adipose tissue -- the effect of obesity and diet-induced weight loss. Int J Obes (Lond) 2013;37:651-657.

34 Nimitphong H, Holick MF, Fried SK, Lee MJ: 25-hydroxyvitamin D_3 and 1,25-dihydroxyvitamin D_3 promote the differentiation of human subcutaneous preadipocytes. PLoS One 2012;7:e52171.

35 Dahl RC: Establishment of an adipocyte cell-based model to investigate the effect of short-chain fatty acids, especially butyrate, on insulin sensitivity and glucose homeostasis in fat tissue. Thesis - Aarhus University, Faculty of Science and Technology, Department of Animal Science, Denmark, 2013.

36 Zhang Z, Zhang H, Hu Z, Wang P, Wan J, Li B: Synergy of 1,25-dihydroxyvitamin D3 and carboplatin in growth suppression of SKOV-3 cells. Oncol Lett 2014;8:1348-1354.

37 Li HX, Gao JM, Liang JQ, Xi JM, Fu M, Wu YJ: Vitamin D3 potentiates the growth inhibitory effects of metformin in DU145 human prostate cancer cells mediated by AMPK/mTOR signalling pathway. Clin Exp Pharmacol Physiol 2015;42:711-717.

38 Pickholtz I, Saadyan S, Keshet GI, Wang VS, Cohen R, Bouwman P, Jonkers J, Byers SW, Papa MZ, Yarden RI: Cooperation between BRCA1 and vitamin D is critical for histone acetylation of the p21waf1 promoter and growth inhibition of breast cancer cells and cancer stem-like cells. Oncotarget 2014;5:11827-11846.

39 Bao A, Li Y, Tong Y, Zheng H, Wu W, Wei C: 1,25-Dihydroxyvitamin D_3 and cisplatin synergistically induce apoptosis and cell cycle arrest in gastric cancer cells. Int J Mol Med 2014;33:1177-1184.

40 Tchkonia T, Morbeck DE, Von Zglinicki T, Van Deursen J, Lustgarten J, Scrable H, Khosla S, Jensen MD, Kirkland JL: Fat tissue, aging, and cellular senescence. Aging Cell 2010;9:667-684.

41 Ali AT, Hochfeld WE, Myburgh R, Pepper MS: Adipocytes and adipogenesis. Eur J Cell Biol 2013;92:229-236.

42 Pawlikowski JS, Adams PD, Nelson DM: Senescence at a glance. J Cell Sci 2013;126:4061-4067.

43 Mota de Sá P, Richard AJ, Hang H, Stephens JM: Transcriptional regulation of adipogenesis. Compr Physiol 2017;7:635-674.

44 Choi KM, Lee YS, Sin DM, Lee S, Lee MK, Lee YM, Hong JT, Yun YP, Yoo HS: Sulforaphane inhibits mitotic clonal expansion during adipogenesis through cell cycle arrest. Obesity (Silver Spring) 2012;20:1365-1371.